Am J Cancer Res 2022;12(4):1535-1555
www.ajcr.us /ISSN:2156-6976/ajcr0134763

Original Article

β-elemene suppresses tumor metabolism and stem cell-like properties of non-small cell lung cancer cells by regulating PI3K/AKT/mTOR signaling

Guangyu Cheng[1], Lin Li[2], Qingjie Li[1], Shulin Lian[3], Hongbo Chu[1], Yunlu Ding[1], Chikun Li[1], Yan Leng[4]

[1]Research Center, Affiliated Hospital to Changchun University of Chinese Medicine, Jilin 130021, China; [2]Department of Health Care, Affiliated Hospital to Changchun University of Chinese Medicine, Jilin 130021, China; [3]Department of Surgery, Affiliated Hospital to Changchun University of Chinese Medicine, Jilin 130021, China; [4]Department of Encephalopathy, Affiliated Hospital to Changchun University of Chinese Medicine, Jilin 130021, China

Received April 28, 2021; Accepted March 16, 2022; Epub April 15, 2022; Published April 30, 2022

Abstract: Multi-drug resistance remains a critical issue in cancer treatment that hinders the effective use of chemotherapeutic drugs. The active components of traditional Chinese medicine have been applied as adjuvants to accentuate the anticancer properties of conventional drugs such as cisplatin. However, their application requires further validation and optimization. This study explored the anticancer activity of β-elemene, a natural component of traditional Chinese medical formulations. The effect of β-elemene on the anticancer properties of cisplatin was evaluated in A549 and NCI-H1650 lung cancer cells. Cell apoptosis, stem-like properties, glucose metabolism, multi-drug resistance, and PI3K/AKT/mTOR activation were assessed via flow cytometry, tumorsphere formation, and western blotting. The target genes of β-elemene were predicted using bioinformatics tools and validated in both cell lines. A xenograft model of lung cancer was established in nude mice to evaluate the combined effects of β-elemene and cisplatin *in vivo*. We found that β-elemene acted synergistically with cisplatin against non-small cell lung cancer cells by promoting apoptosis and impairing glucose metabolism, multi-drug resistance, and stemness maintenance. These effects were mediated by the inhibition of PI3K/AKT/mTOR activation. Bioinformatics analysis revealed that RB1 and TP53 are common target genes associated with lung cancer and β-elemene. The antitumorigenic properties of β-elemene were confirmed *in vivo*, wherein β-elemene, along with cisplatin, significantly suppressed tumor growth in a mouse xenograft model of non-small cell lung cancer. As such, β-elemene acted as an inhibitor of PI3K/AKT/mTOR signaling and enhanced the anticancer effect of cisplatin by targeting tumor metabolism, chemoresistance, and stem-like behavior. Thus, β-elemene is an effective anticancer adjuvant agent with potential clinical applications.

Keywords: Lung cancer, β-elemene, multi-drug resistance, Warburg effect, cancer stem cell, apoptosis

Introduction

Lung cancer accounts for approximately 25% of global cancer-related deaths and was the main cause of cancer-related deaths in 2018 [1]. It can be subdivided into small cell and non-small cell lung cancers (NSCLCs), which account for approximately 20% and 80% of lung cancer cases, respectively [2]. At diagnosis, most patients with lung cancer are at an advanced stage [3]. Cytotoxic chemotherapy is an effective option for these patients, but the 12-month overall survival rate is low, while the five-year survival rate is only 10% [4]. Currently, the efficacy of chemotherapy and targeted therapy is only 20%-30% as lung cancer is highly prone to treatment failure due to multi-drug resistance (MDR), tumor metastasis, and recurrence. Therefore, understanding the mechanisms underlying chemoresistance has become an important goal in the clinical treatment of lung cancer. While research on MDR has progressed, the molecular and genetic basis of MDR is complex and involves multiple processes, such as drug transport, drug metabolism, cell survival, repair, and apoptosis [5]. However,

many of the specific molecular mechanisms are still not fully understood.

Cancer stem cells (CSCs) are small subpopulations of cancer cells that can self-renew and develop into tumors [6]. Their existence explains not only the possible causes of tumorigenesis but also the mechanisms of heterogeneity, metastasis, recurrence, and MDR in tumors [6-8]. In recent years, studies have found that CSCs contribute to tumor angiogenesis, MDR, and metastasis. Therefore, the discovery of drugs that target CSCs so that tumors can be controlled during the developmental stage is of great significance for the clinical treatment of lung cancer. Additionally, tumor cells exhibit different metabolic behaviors compared to normal cells, and this phenomenon also contributes to cancer progression. In most tumor or highly proliferating cells, glucose does not enter the mitochondria as it is produced by pyruvate but is converted to lactic acid by lactate dehydrogenase (LDH). Even under adequate oxygen conditions, cancer cells preferentially decompose glucose to lactic acid, a process called “aerobic glycolysis” or the Warburg effect [9]. The Warburg effect is a form of metabolic reprogramming that correlates with the occurrence and development of tumors. Studies have corroborated that the Warburg effect is related to changes in the tumor microenvironment, adaptation to hypoxic conditions, oncogene activation, inactivation of tumor suppressor genes, mitochondrial function, and abnormal expression of glucose metabolism enzymes. These factors are conducive to the growth of tumor cells, which helps them escape apoptosis and promote tumor metastasis. In particular, the phosphatidylinositol-4,5-bisphosphate 3-kinase/protein kinase B/mammalian target of rapamycin (PI3K/AKT/mTOR) pathway is abnormally activated in a variety of tumor cells, including in lung cancer. PI3K/AKT/mTOR signaling mediates the occurrence, development, metabolism, and drug resistance of tumor cells [10], and is thus a significant target in cancer therapies.

In recent years, the use of traditional Chinese medicine (TCM) as a complementary means of chemotherapeutic intervention has attracted increasing attention from cancer researchers. A variety of natural or herbal compounds have been applied in TCM, and they have been shown to either target tumor cells directly or enhance the therapeutic effect of existing clinical drugs. Elemene, a terpene compound extracted from the genus Zingiberaceae [11], is marketed as a national second-class broad-spectrum antitumor drug. The four subtypes of elemene (α, β, γ, and δ) are structural isomers, with β-elemene (1-methyl-2,4-di(prop-1-en-2-yl)-1-vinylcyclohexane) being the main subtype [12, 13]. β-elemene possesses the unique ability to penetrate the blood-brain barrier [14, 15]; thus, it has been applied in the treatment of malignant pleural effusions [16] and metastatic cancers, including acute myeloid leukemia [17], ovarian cancer [18], and breast cancer [19]. As a natural plant extract, β-elemene causes few adverse reactions and has been applied in hyperthermia therapy and radiotherapy for NSCLC [20, 21]. β-elemene exerts its antitumor effect by inducing apoptosis, arresting the cell cycle, reversing MDR, and inhibiting tumor cell proliferation [22, 23] via inhibition of PI3K/AKT/mTOR signaling [24]. Simultaneously, β-elemene inhibited the proliferation of gastric CSCs and increased their sensitivity to temozolomide [25]. However, in NSCLC, whether β-elemene inhibits CSCs and, in particular, whether it disrupts the metabolic reprogramming of tumor cells, thereby improving their chemosensitivity of tumor cells, remains to be investigated.

This study was performed based on the hypothesis that β-elemene exerts antitumor effects by inhibiting PI3K/AKT/mTOR signaling, thereby affecting MDR, stemness, and metabolic reprogramming of tumor cells to enhance chemosensitivity. The therapeutic effect of β-elemene and its mechanism of action on NSCLC were investigated *in vitro* and *in vivo*, and the potential target genes of β-elemene were examined by Gene Ontology and Kyoto Encyclopedia of Genes and Genomes analyses with the aim of advancing the application of TCM in cancer treatment.

Materials and methods

Materials

The human NSCLC cell lines, A549 and NCI-H1650, were obtained from the Cell Bank of the Chinese Academy of Sciences (Shanghai, China). β-Elemene (product code: C5505) was purchased from Apexbio (Boston, MA), cisplatin

(product code: P4394) from Sigma-Aldrich (St. Louis, MO), and 2-deoxy-D-glucose (2-DG; product code: D109194) from Aladdin (Shanghai, China). PI3K inhibitor LY294002; (product code: S1105), AKT inhibitor GSK690693 (product code: S1113), and mTOR inhibitor AZD8055 (product code: S1555) were obtained from Selleck Chemicals (Houston, TX, USA).

Cell culture and drug treatment

A549 cells were cultured in Ham's F-12K medium and NCI-H1650 cells were cultured in RPMI-1640 medium, both containing 10% fetal bovine serum and 1% penicillin-streptomycin at 37°C in an incubator containing 5% CO_2. The cells were passaged when they reached 90% confluence. For each assay, cells were treated for 24 h with 10 μM cisplatin and/or 3 μg/mL β-elemene (**Figure 1A**) or at the indicated concentrations. For experiments involving inhibitors of PI3K (50 μM), AKT (10 μM), or mTOR (10 μM), the inhibitors were added 6 h prior to the addition of β-elemene. 2-DG was administered at a concentration of 10 mM for 48 h. Each experiment was performed in triplicate.

Evaluation of cell growth and drug sensitivity

Cell Counting kit-8 (CCK-8) was used to evaluate cell survival and proliferation. A549 and NCI-H1650 cells were resuspended in their respective growth mediums and seeded in a 96-well plate at a density of 5×10^3 cells/well. After 24 h of treatment with cisplatin (10 μM) or β-elemene (2.5, 5, 10, 20, or 40 μg/mL), 10 μL of CCK-8 reagent (CA1210, Solarbio, Beijing, China) was added to each well, and the cells were further incubated for 4 h. Absorbance at 450 nm was measured using a microplate reader (Multiskan FC, Thermo) and the relative viability was calculated. The 3-(4,5-dimethylthiazol-2-yl)-2,5-diphenyltetrazolium bromide (MTT) assay was conducted to assess the sensitivity of A549 and NCI-H1650 cells to cisplatin and β-elemene. Cells in their logarithmic phase of growth were resuspended in growth medium and seeded in a 96-well plate at a density of 5×10^3 cells/well (180 μL in each well). After overnight incubation at 37°C in 5% CO_2, the cells were treated for 24 h with cisplatin (2, 5, 10, 20, or 50 μM), with or without the addition of 3 μg/mL β-elemene. Thereafter, 20 μL of MTT reagent (5 mg/mL; product code: C1736, Bioswamp, Myhalic Biotechnology Co., Ltd., Wuhan, China) was added to each well, and the cells were cultured for 4 h. The medium was removed, and 150 μL of dimethyl sulfoxide was added to each well, after which the plate was shaken for 10 min. The absorbance of each well was obtained using a microplate reader (Multiskan FC) at 490 nm.

Flow cytometry

Flow cytometry was performed to detect apoptosis and assess the CSC population. For apoptosis, the Annexin V-fluorescein isothiocyanate (FITC)/propidium iodide (PI) apoptosis detection kit (556547, BD Biosciences) was used. After the cells were treated with cisplatin and/or β-elemene as indicated, they were washed with phosphate-buffered saline (PBS) and trypsinized. The cells were then transferred to Eppendorf tubes and centrifuged for 5 min, after which the supernatants were removed. Next, 1×10^6 cells were resuspended and centrifuged for 5 min, and the supernatant was collected, after which the cells were resuspended in 1 mL of pre-cooled PBS. After gentle shaking, the cells were centrifuged at 1000 × g at 4°C for 5 min and the supernatant was removed. This step was repeated three times, and the cells were finally resuspended in 200 μL binding buffer. Thereafter, Annexin V-FITC and PI (10 μL each) were added to the cells and gently mixed. The cells were incubated for 30 min in the absence of light at 4°C, and a further 300 μL of binding buffer was added, after which the cells were immediately subjected to flow cytometry. To assess the proportion of the CSC subpopulation, 1×10^6 treated cells were resuspended in 100 μL of flow cytometry buffer in an Eppendorf tube. In each tube, 2 μL of phycoerythrin-cyanine 7-conjugated CD133 monoclonal antibody (25-1339-42, eBioscience) and 2 μL of fluorescein isothiocyanate-conjugated CD44 monoclonal antibody (11-0441-82, eBioscience) were added and the cells were incubated at 4°C for 30 min in the dark. The cells were then washed once with 2 mL of flow cytometry buffer and centrifuged at 1500 rpm at 4°C for 5 min. The cells were resuspended and analyzed by flow cytometry.

Tumorsphere formation assay

A549 and NCI-H1650 cells were treated as indicated, trypsinized, resuspended, and centrifuged for 3 min at 1000 rpm. The superna-

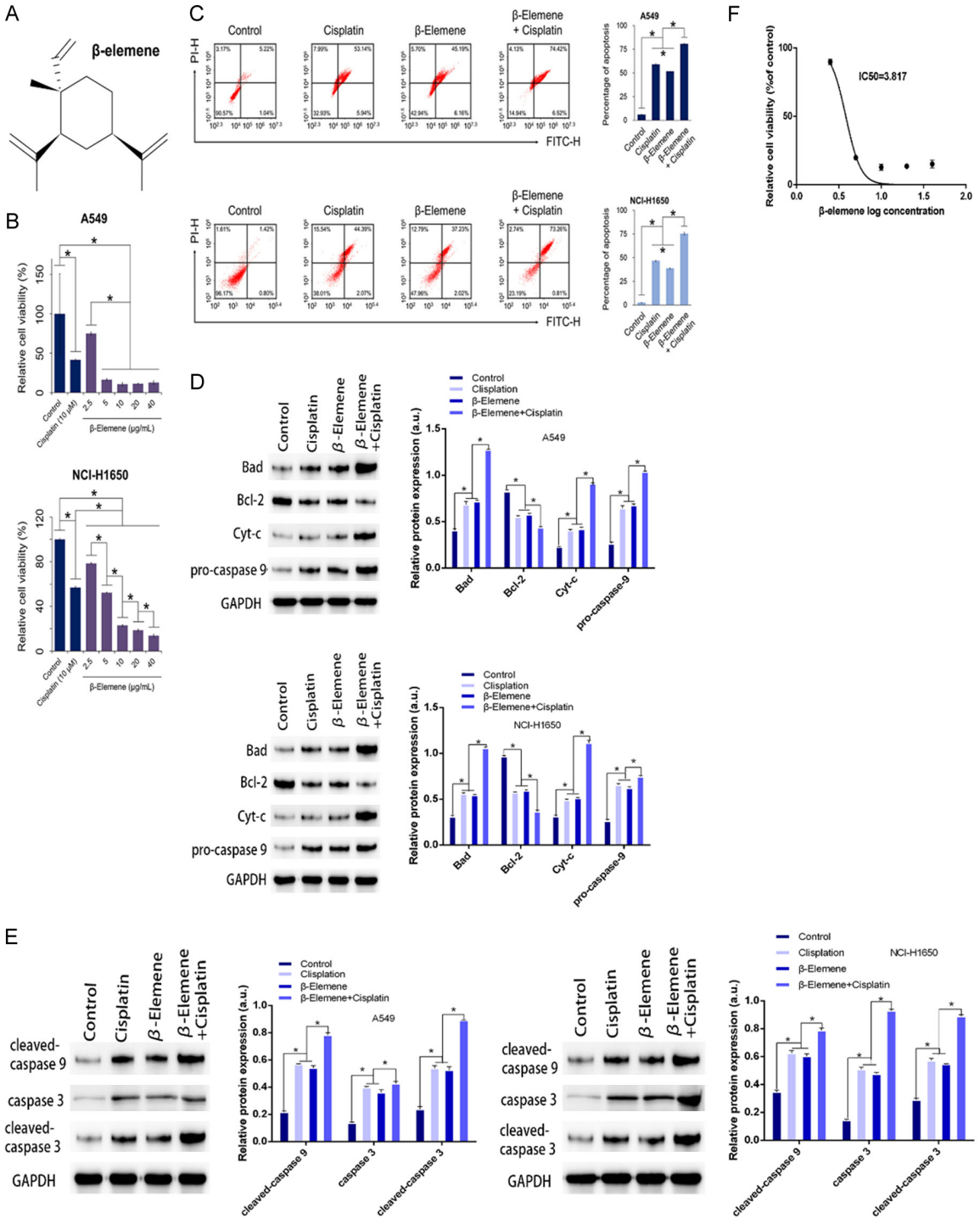

Figure 1. Effect of β-elemene on the survival and apoptosis of A549 and NCI-H1650 cells. A. Molecular structure of β-elemene. B. CCK-8 assay of the viability of A549 and NCI-H1650 cells after treatment with 10 μM cisplatin or β-elemene at 2.5, 5, 10, 20, or 40 μg/mL for 24 h. C. Flow cytometry of A549 and NCI-H1650 cell apoptosis after treatment with 10 μM cisplatin and/or 3 μg/mL β-elemene for 24 h. Early apoptotic cells are shown in the bottom right quadrant and late apoptotic cells are shown in the top right quadrant. Bar graphs represent the sum of the percentages of early and late apoptotic cells. D. Western blot and quantification of the expression of apoptosis-related proteins (Bcl-2, Bad, Cyt-c, and pro-caspase 9) in A549 and NCI-H1650 cells treated with 10 μM cisplatin and/or 3 μg/mL β-elemene for 24 h. E. Western blot and quantification of the expression of apoptosis-related proteins (cleaved-caspase 9, caspase 3 and c-caspase 3) in A549 and NCI-H1650 cells treated with 10 μM cisplatin and/or 3 μg/mL β-elemene for 24 h. F. The IC50 of cisplatin measured after β-elemene treatment. The data represent the mean ± SD (n = 3), *P < 0.05.

tant was removed, and the cells were washed twice with PBS. The cells were then resuspended in a medium consisting of 10 μg/mL transferrin (PE1717, Bioswamp), 5 μg/mL insulin (I8040, Solarbio), 20 ng/mL basic fibroblast growth factor (100-18B, Peprotech), 20 ng/mL epidermal growth factor (AF-100-15, Peprotech), and 2% B27 (17504044, Gibco), and inoculated in a 6-well plate at a concentration of 1×10^5 cells/mL. After seven days, images of the resulting tumorspheres were obtained using an optical microscope (DMIL LED, Leica).

Quantitative reverse transcription polymerase chain reaction (qRT-PCR)

RNA was extracted from A549 and NCI-H1650 cells using TRIzol reagent (15596026, Ambion, Inc., Foster City, CA, USA). The RevertAid First Strand cDNA Synthesis Kit (K1622, Thermo Scientific) was used to reverse transcribe the cDNA. The SYBR Green PCR kit (KM4101; KAPA Biosystems, Wilmington, MA, USA) was used to perform qRT-PCR. The primer sequences were as follows: RB1 forward, 5'-AACACCACGAAAAAGTAAC-3' and reverse, 5'-GTAATACAAGCGAACTCC-3'; TP53 forward, 5'-TGCGTGTGGAGTATTTGG-3' and reverse, 5'-GATTCTCTTCCTCTGTGCG-3'; and GAPDH forward, 5'-CCACTCCTCCACCTTTG-3' and reverse, 5'-CACCACCCTGTTGCTGT-3'. The experimental conditions were as follows: initial denaturation at 95°C for 3 min; 40 cycles of denaturation at 95°C for 5 s, annealing at 56°C for 10 s, an extension at 72 for 25 s; and a final extension at 65°C for 5 s and 95°C for 50 s. Data were analyzed using the $2^{-\Delta\Delta Ct}$ method.

Western blot

Cell or tissue samples were lysed using a radioimmunoprecipitation assay buffer. A bicinchoninic acid assay kit (W1712; Bioswamp) was used to quantify the extracted proteins. For sodium dodecyl sulfate-polyacrylamide gel electrophoresis, 20 μg of protein was added to each lane. The separated proteins were transferred onto polyvinylidene fluoride membranes. Blocking was performed by incubating the membranes in 5% skim milk at room temperature for 2 h. Thereafter, the membranes were incubated overnight at 4°C with primary antibodies (all obtained from Bioswamp) against Bcl-2 (1:1000, PAB31568), Bad (1:200, PAB36687), cytochrome-c (Cyt-c, 1:1000, PAB30480), pro-caspase 9 (1:1000, MAB43790), octamer-binding transcription factor 4 (OCT4, 1:1000, PAB35586), sex-determining region Y-box 2 (SOX2, 1:1000, PAB30154), Nanog (1:1000, PAB33609), glucose transporter 1 (GLUT1, 1:1000, PAB30639), hexokinase 1 (HK1, 1:1000, PAB30519), lactate dehydrogenase A (LDHA, 1:1000, PAB30703), p-glycoprotein (pgp, 1:1000, PAB36768), ABCB2 (1:1000, PAB41957), ATP-binding cassette super-family G member 2 (ABCG2, 1:1000, PAB38421), MDR (1:1000, PAB32152), phosphorylated (p)-PI3K (1:1000, PAB43641-P), PI3K (1:1000, MAB37566), p-AKT (1:1000, PAB43181-P), AKT (1:1000, PAB30596), p-mTOR (1:1000, PAB36313-P), mTOR (1:1000, PAB33332), retinoblastoma protein (pRb, 1:1000, PAB36408), p53 (1:1000, PAB30082), and GAPDH (1:1000, PAB36269). Three washes were performed with PBS/Tween 20 for 5 minutes each. Membranes were incubated with goat anti-rabbit IgG (1:20000, SAB43714) for 1 h at room temperature. The membranes were washed three times with PBS/Tween 20 for 5 min each and subjected to enhanced chemiluminescence detection (WBKLS0010, Millipore). The relative values of the protein bands were analyzed based on intensity using the Tanon GIS software.

In vivo studies

All animal experiments were approved and performed in accordance with the guidelines of the Animal Care and Welfare Committee of Changchun University of Chinese Medicine (approval no. 20181021). A subcutaneous lung tumor xenograft model was established in mice using A549 cells. Male BALB/c-nu mice (aged 4-5 weeks) were acquired from Beijing HFK Bioscience Co., Ltd. (Beijing, China) and housed under specific pathogen-free conditions. After seven days of adaptive feeding, the mice were anesthetized with 30 mg/kg sodium pentobarbital, and 1×10^7 A549 cells in the logarithmic growth phase were injected subcutaneously into the upper right axilla of the mice. When the tumors reached a volume of 3 mm^3, the mice were divided into four groups (n = 6 per group) and subjected to the following treatments: control (intraperitoneal injection of physiological saline), cisplatin (oral gavage at 5 mg/kg once every three days for three weeks), β-elemene (intraperitoneal injection at 5 mg/

kg once daily for seven days), and a combination of β-elemene and cisplatin. During the experimental period, the tumor weight was measured daily. Tumor length (L) and width (W) were measured every alternate day, and the tumor volume was calculated as $L \times W^2/2$. After 28 days, the mice were sacrificed using an overdose of sodium pentobarbital and the tumors were extracted for further evaluation.

Network pharmacology analysis of potential target genes of β-elemene

Based on the Traditional Chinese Medicine Systems Pharmacology (TCMSP) database and analysis platform, the target genes of β-elemene were screened. The full names of the target proteins were matched to gene symbols (UniProtID) in the UniProt database (https://www.uniprot.org/). Twenty-five β-elemene targets were selected and transformed into Entrez IDs according to the gene symbol. Lung cancer-related targets were identified using the OMIM, DiGSeE, and GenCliP databases and a Venn diagram was generated to illustrate the common targets among the three. These common target genes were compared with those of β-elemene previously identified using TCMSP, and a Venn diagram was generated to reveal the common targets of lung cancer and β-elemene.

Statistical analysis

Statistical analysis was performed using OriginPro 8. One-way analysis of variance followed by Tukey's post-hoc test was performed to assess the differences between more than two groups. Data represent the mean ± standard deviation (SD) of three (*in vitro*) or six (*in vivo*) independent replicates. Statistical significance was set at $P < 0.05$.

Results

β-elemene enhanced the anticancer properties of cisplatin

A549 and NCI-H1650 cells were treated with 10 μM cisplatin or β-elemene at 2.5, 5, 10, 20, or 40 μg/mL for 24 h, and cell viability was measured using the CCK-8 assay (**Figure 1B**). Compared with untreated cells (control), cisplatin significantly decreased cell viability ($P < 0.05$). β-elemene did not affect A549 cell viability at 2.5 μg/mL but showed a prominent inhibitory effect from 5 μg/mL onward ($P < 0.05$), with no differences between 5, 10, 20, and 40 μg/mL. For NCI-H1650 cells, cell viability decreased in a dose-dependent manner upon β-elemene treatment ($P < 0.05$), and the effect of β-elemene at 5 μg/mL matched that of 10 μM cisplatin; the IC50 was determined to be 3.817 after β-elemene intervention (**Figure 1F**). A549 and NCI-H1650 cells were subjected to individual treatment with 10 μM cisplatin and 3 μg/mL β-elemene or co-treatment with both drugs, and cell apoptosis was determined after 24 h (**Figure 1C**). Individually, cisplatin and β-elemene induced a considerable increase in late apoptosis compared to that in non-treated cells. However, the co-administration of the drugs promoted apoptosis to a greater extent. Evaluation of the expression of apoptosis-related proteins (**Figure 1D** and **1E**) revealed that the anti-apoptotic Bcl-2 was significantly downregulated ($P < 0.05$) by individual cisplatin or β-elemene administration, while the pro-apoptotic Bad, Cyt-c, cleaved-caspase 9, caspase 3, c-caspase 3, and pro-caspase 9 were upregulated ($P < 0.05$). In addition, co-treatment with cisplatin and β-elemene accentuated the pro-apoptotic effect of individual treatments ($P < 0.05$) in both cell types, demonstrating that β-elemene enhanced the anticancer property of cisplatin *in vitro*.

Cisplatin-induced disruption of stemness maintenance and glucose metabolism was further promoted by β-elemene

The proportion of CSCs in the A549 and NCI-H1650 cell populations was assessed by CD133/CD44 [26] double labeling via flow cytometry after the cells were treated with 10 μM cisplatin and/or 3 μg/mL β-elemene for 24 h (**Figure 2A**). The ability of the cells to form tumorspheres was examined microscopically as a further indication of the presence of CSCs (**Figure 2B**). By calculating the tumor sphere formation rate, it was found that non-treated (control) cells readily aggregated to form tumorspheres, whereas individual administration of 10 μM cisplatin or 3 μg/mL β-elemene greatly reduced the size of the assembled tumorspheres in both cell types. When β-elemene was co-administered with cisplatin, tumorsphere formation was severely disrupted, as demonstrated by sparse clusters and failure to

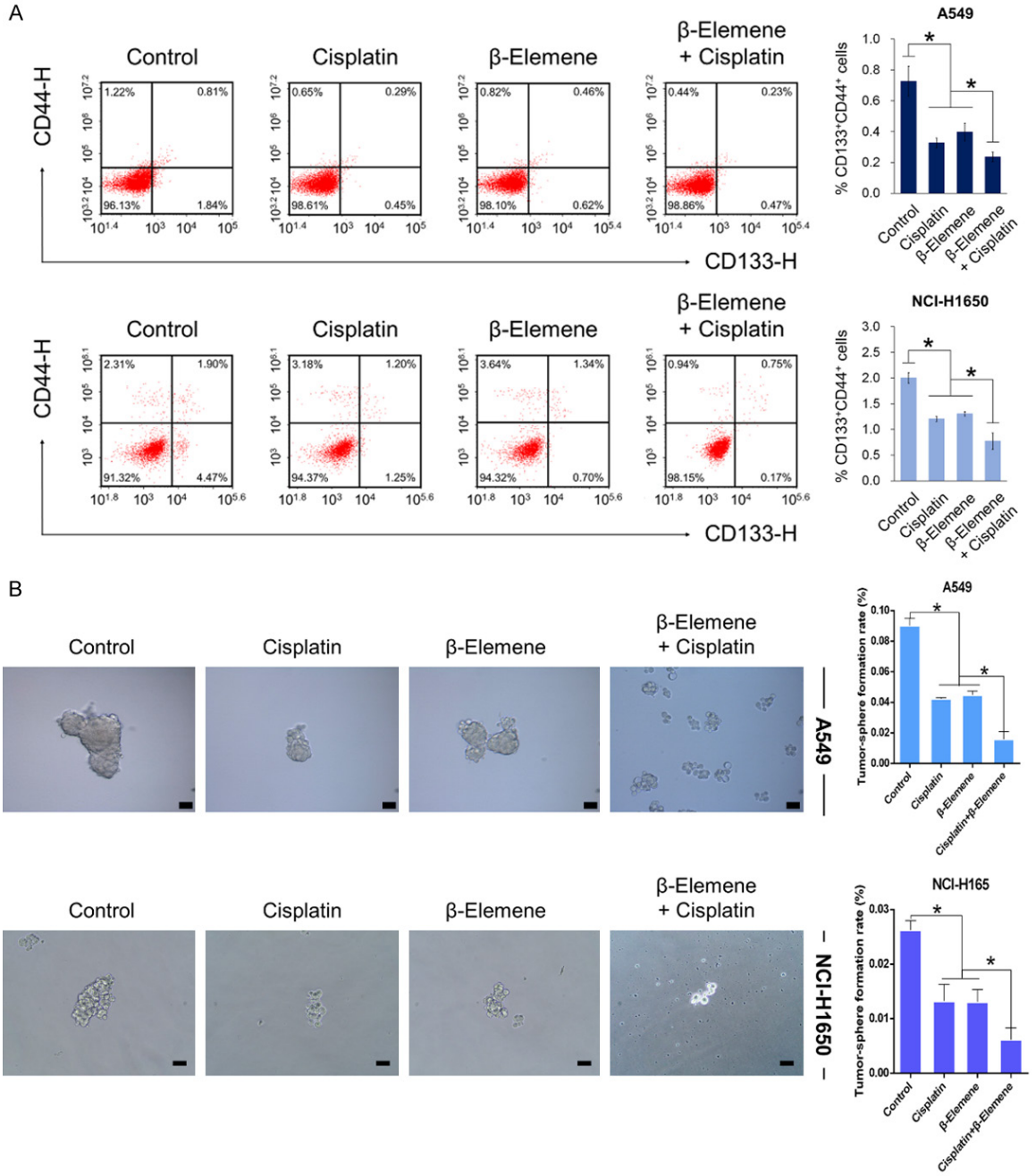

Figure 2. Effect of β-elemene on stemness maintenance and tumorsphere formation in A549 and NCI-H1650 cells. A. Flow cytometry to determine the proportion of CSCs in A549 and NCI-H1650 cells treated with 10 μM cisplatin and/or 3 μg/mL β-elemene for 24 h. Bar graphs represent the percentage of CD133+/CD44+ cells, which are shown in the top right quadrant of the dot plots. B. Tumorsphere formation ability of A549 and NCI-H1650 cells treated with 10 μM cisplatin and/or 3 μg/mL β-elemene for 24 h. Scale bar = 50 μm. The data represent the mean ± SD (n = 3), *P < 0.05.

form large aggregates. Western blotting was performed to evaluate the expression of proteins associated with stemness maintenance, namely OCT4, SOX2, and Nanog (**Figure 3A**). In this study, individual cisplatin or β-elemene treatment induced significant downregulation of these stemness markers ($P < 0.05$), and the effects of these two drugs were similar. However, when administered together, cisplatin and β-elemene downregulated the stem-

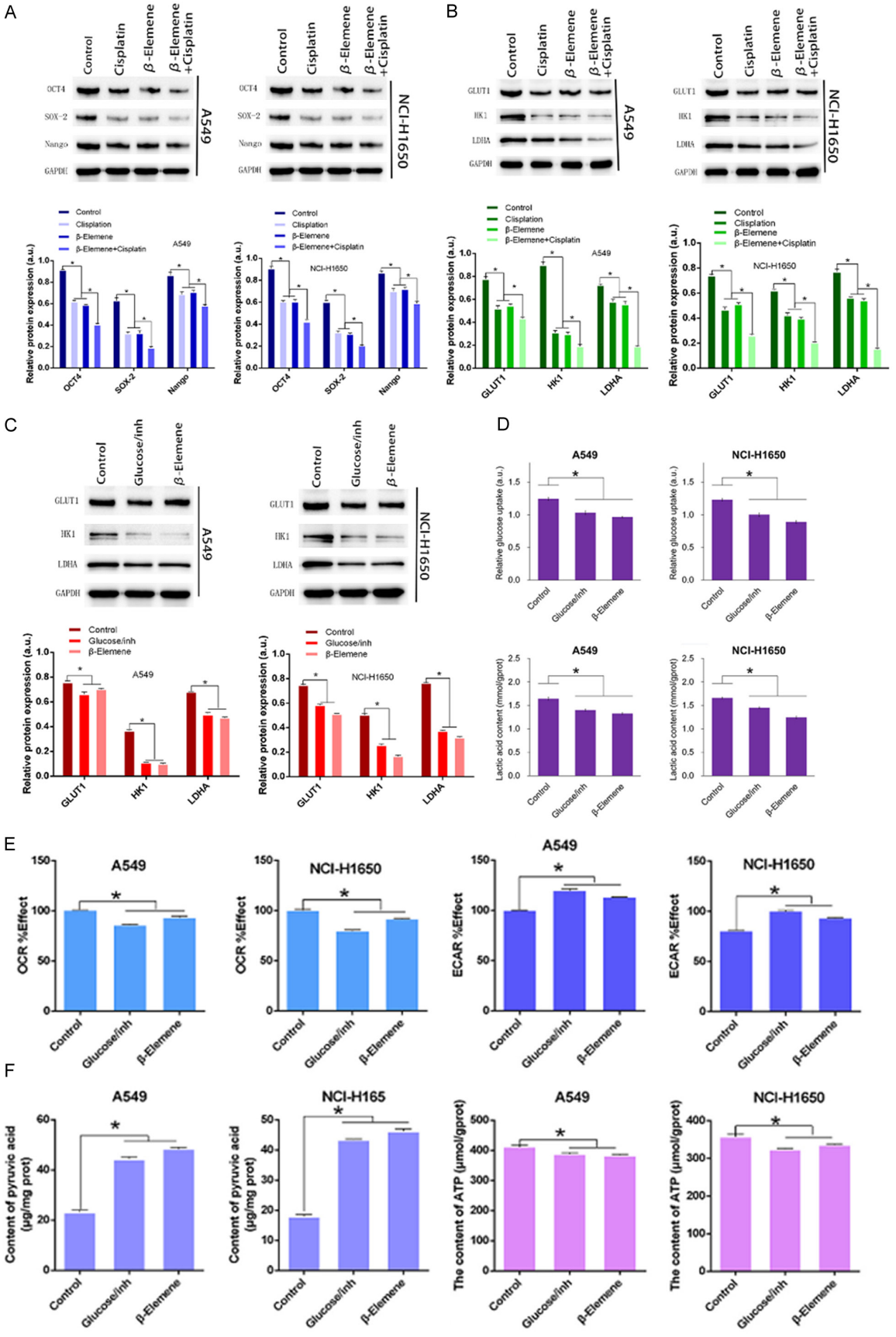
A
Control
Cisplatin
β-Elemene
β-Elemene +Cisplatin
OCT4
SOX-2
Nango
GAPDH
A549
NCI-H1650
Control
Clisplation
β-Elemene
β-Elemene+Cisplatin
Relative protein expression (a.u.)
OCT4
SOX-2
Nango
B
GLUT1
HK1
LDHA
GAPDH
GLUT1
HK1
LDHA
C
Control
Glucose/inh
β-Elemene
D
Relative glucose uptake (a.u.)
Lactic acid content (mmol/gprot)
E
OCR %Effect
ECAR %Effect
F
Content of pyruvic acid (μg/mg prot)
The content of ATP (μmol/gprot)
NCI-H165

Figure 3. Effect of β-elemene on stemness maintenance and glucose metabolism in A549 and NCI-H1650 cells. Western blot and quantification of the expression of (A) stemness maintenance markers (OCT4, SOX2, and Nanog) and (B) proteins related to glucose metabolism (GLUT1, HK1, and LDHA) in A549 and NCI-H1650 cells treated with 10 μM cisplatin and/or 3 μg/mL β-elemene for 24 h. (C) Western blot and quantification of the expression of proteins relevant to glucose metabolism (GLUT1, HK1, and LDHA) in A549 and NCI-H1650 cells treated with 3 μg/mL β-elemene for 24 h or 10 mM 2-DG (glucose inhibitor) for 48 h. (D) Glucose uptake and lactic acid content in A549 and NCI-H1650 cells treated with 3 μg/mL β-elemene for 24 h or 10 mM 2-DG (glucose inhibitor) for 48 h. (E) OCR and ECAR detection by Fluorescent. (F) ATP and pyruvate content by biochemical assay. The data represent the mean ± SD (n = 3), *P < 0.05.

ness markers to a greater extent than the individual components (P < 0.05). These findings indicate that β-elemene enhances the ability of cisplatin to impair CSC function and inhibit stemness maintenance in both A549 and NCI-H1650 cells.

As an indicator of tumor metabolism, glucose uptake and metabolism were examined in A549 and NCI-H1650 cells. The individual administration of cisplatin or β-elemene significantly suppressed the expression of proteins associated with glucose metabolism (P < 0.05), namely GLUT1, HK1, and LDHA (**Figure 3B**), and this inhibitory effect was attenuated by the co-administration of the drugs (P < 0.05). Furthermore, the effect of 3 μg/mL β-elemene was similar to that of 10 nM 2-DG (a glucose inhibitor), as measured by inhibition of GLUT1, HK1, and LDHA in A549 and NCI-H1650 cells (**Figure 3C**). Concurrently, we showed that β-elemene reduced the relative glucose intake and lactic acid production in A549 and NCH-H1650 cells (P < 0.05), similar to 2-DG (**Figure 3D**). At the same time, the oxygen consumption rate (OCR) decreased (P < 0.05) and the extracellular acidification rate (ECAR) increased (P < 0.05) in A549 and NCH-H1650 cells (**Figure 3E**). Assaying pyruvate in the mitochondria and ATP concentration in cells (**Figure 3F**), β-elemene decreased the levels of pyruvate and ATP in both A549 and NCH-H1650 cells (P < 0.05). These observations imply that β-elemene itself may act as a glucose inhibitor and that its action in enhancing the function of cisplatin could be related to the disruption of tumor glucose metabolism and suppression of the Warburg effect.

β-Elemene enhanced the chemosensitivity of A549 and NCI-H1650 cells to cisplatin by regulating PI3K/AKT/mTOR signaling

An MTT assay was performed to evaluate the sensitivity of A549 and NCI-H1650 cells to cisplatin at various concentrations, with or without co-administration of 3 μg/mL β-elemene for 24 h (**Figure 4A**). Cisplatin alone induced a dose-dependent decrease in the viability of both cell types at concentrations up to 50 μM (P < 0.05). The same phenomenon was observed with β-elemene co-administration at cisplatin concentrations of 2-50 μM (P < 0.05). However, a significant decrease in viability was observed at each cisplatin concentration when compared to that of 0 μM β-elemene (P < 0.05), indicating that β-elemene effectively increased the sensitivity of A549 and NCI-H1650 cells to cisplatin. Next, the expression of proteins associated with MDR (P-gp, ABCB2, and ABCG2) was detected by western blotting after A549 and NCI-H1650 cells were treated with cisplatin at 0, 2, 5, 10, 20, or 50 μM, in the presence or absence of 3 μg/mL β-elemene (**Figure 4B**). In A549 cells, the difference between 0 and 3 μg/mL β-elemene was evident at a cisplatin concentration of 5 μM for P-gp and ABCB2, and 2 μM for ABCG2 (P < 0.05). In the absence of β-elemene, cisplatin exerted an inhibitory effect on P-gp at 20 μM and on ABCB2 and ABCG2 at 50 μM (P < 0.05, compared with non-treated cells). In NCI-H1650 cells, the difference between 0 and 3 μg/mL β-elemene was evident at a cisplatin concentration of 2 μM for ABCB2 and ABCG2 and 0 μM for P-gp (P < 0.05). In the absence of β-elemene, cisplatin exerted an inhibitory effect on P-gp, ABCB2, and ABCG2 at 5 μM (P < 0.05, compared to untreated cells). Overall, co-administration of 3 μg/mL β-elemene increased the chemosensitivity of A549 and NCI-H1650 cells to cisplatin (P < 0.05).

To determine the role of the PI3K/AKT/mTOR signaling pathway in the regulation of chemosensitivity by β-elemene, phosphorylation of PI3K, AKT, and mTOR was evaluated in A549 and NCI-H1650 cells (**Figure 4C**). Individual administration of 10 μM cisplatin or 3 μg/mL β-elemene decreased the activation of PI3K/AKT/mTOR signaling to a similar extent by do-

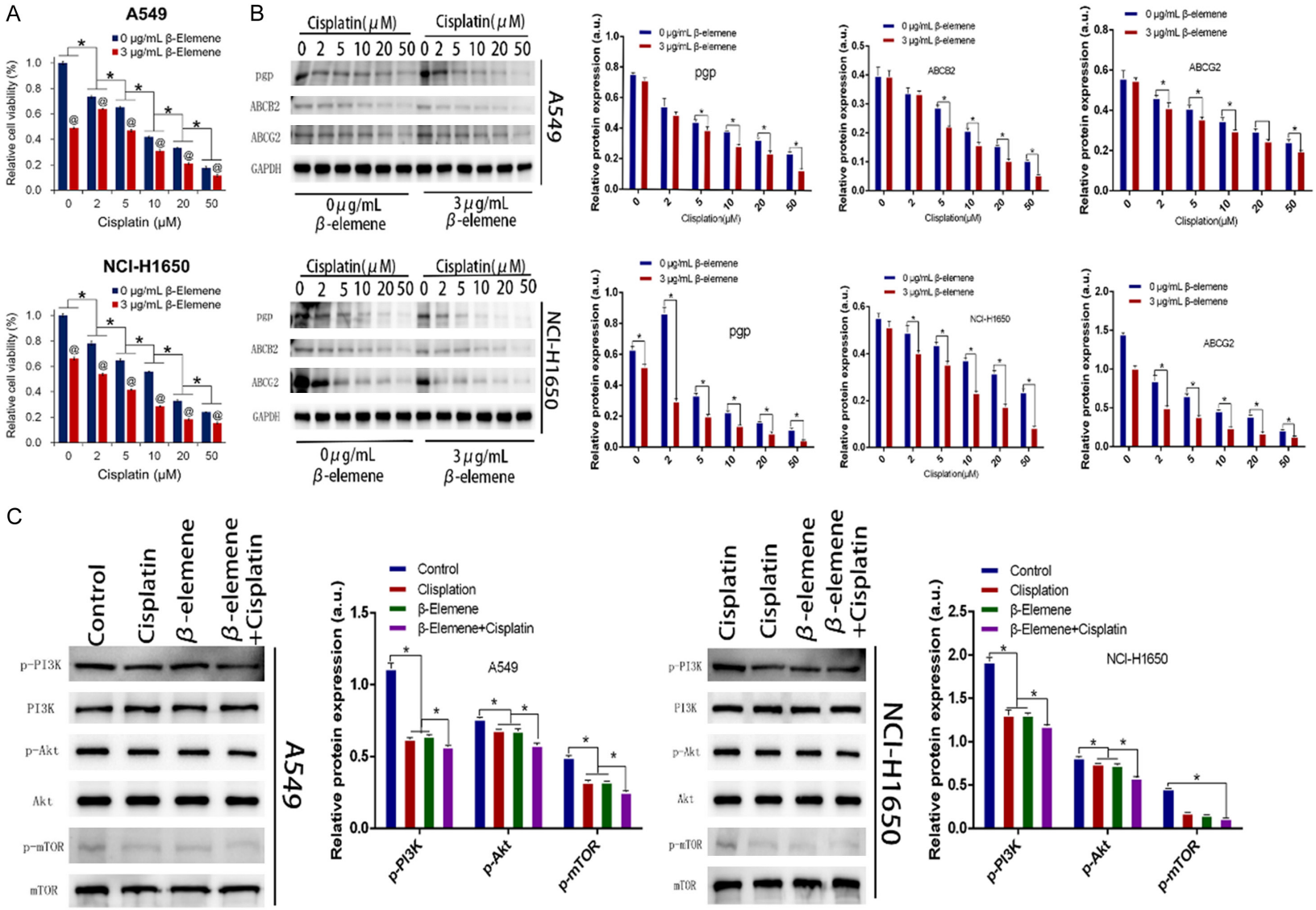

Figure 4. Effect of β-elemene on MDR and PI3K/AKT/mTOR signaling in A549 and NCI-H1650 cells. A. MTT assay of the relative viability of A549 and NCI-H1650 cells after treatment with or without 3 μg/mL β-elemene for 6 h, then with cisplatin at 0, 2, 5, 10, 20, or 50 μM for 24 h. The data represent the mean ± SD (n = 3), *P < 0.05; @P < 0.05 vs. 0 μg/mL β-elemene at same concentration of cisplatin. B. Western blot and quantification of the expression of proteins associated with MDR (pgp, ABCB2, and ABCG2) in A549 and NCI-H1650 cells treated with or without 3 μg/mL β-elemene for 6 h, then with cisplatin at 0, 2, 5, 10, 20, or 50 μM for

24 h. The data represent the mean ± SD (n = 3), *P < 0.05; #P < 0.05 vs. 0 μM cisplatin at the same concentration of β-elemene; ##P < 0.05 vs. 10 μM cisplatin at the same concentration of β-elemene. C. Western blot and quantification of the phosphorylation level of PI3K, AKT, and mTOR relative to total content of respective protein in A549 NCI-H1650 cells treated with 10 μM cisplatin and/or 3 μg/mL β-elemene for 24 h. The data represent the mean ± SD (n = 3), *P < 0.05.

wnregulating the expression of p-PI3K, p-AKT, and p-mTOR relative to the respective total protein content (P < 0.05). However, the combined treatment with the two drugs accentuated this effect by suppressing PI3K/AKT/mTOR phosphorylation (P < 0.05). This observation indicates that β-elemene enhances the regulatory function of cisplatin in PI3K/AKT/mTOR signaling.

PI3K/AKT/mTOR inhibition further promoted the anticancer function of β-elemene

The specific involvement of the PI3K/AKT/mTOR pathway in the action of β-elemene was further investigated via the co-administration of 3 μg/mL β-elemene with inhibitors of PI3K (LY294002, 50 μM), AKT (GSK690693, 10 μM), and mTOR (AZD8055, 10 μM). The effect of the inhibitors on the activation of PI3K/AKT/mTOR was first confirmed by western blot analysis of PI3K, AKT, and mTOR phosphorylation in A549 and NCI-H1650 cells (**Figure 5A**). The ability of A549 and NCI-H1650 cells to form tumorspheres was evaluated after treatment with β-elemene and an inhibitor of PI3K, AKT, or mTOR. As indicated in **Figure 5B**, inhibitors of PI3K/AKT/mTOR greatly reduced the diameter and size of the tumorspheres formed by A549 and NCI-H1650 cells compared to the administration of β-elemene alone. The effect of inhibitor co-administration was similar to that of the β-elemene and cisplatin co-treatment. In terms of apoptosis, co-administration of β-elemene and inhibitors induced a remarkably higher percentage of cell apoptosis than that induced by β-elemene or cisplatin alone (**Figure 5C**). This was complemented by the results of western blotting, which showed that in conjunction with β-elemene, PI3K/AKT/mTOR inhibition further promoted apoptosis by downregulating the anti-apoptotic protein Bcl-2 and upregulating the pro-apoptotic proteins Bad, Cyt-c, and procaspase 9 (**Figure 6**). At the same time, PI3K/AKT/mTOR inhibition suppressed the stem-like and drug-resistant properties of A549 and NCI-H1650 cells, as demonstrated by the downregulation of the stemness markers OCT4, SOX2, and Nanog as well as the MDR protein.

Bioinformatic prediction and preliminary experimental verification of target genes associated with β-elemene and NSCLC

Genes associated with lung cancer were screened using three databases (OMIM, DiGSeE, and GenCliP), and 77 were identified as common among the databases. Additionally, 25 target genes of β-elemene were identified using the TCMSP database (**Table 1**). Venn diagram analysis revealed that there were two common target genes between those identified for lung cancer and β-elemene, namely, RB1 and TP53 (**Figure 7A**). We then carried out a preliminary confirmation of the effect of these target genes in A549 and NCI-H1650 cells by treating them with β-elemene at various concentrations for different durations. The mRNA expression of RB1 and TP53 and the protein expression of pRb and p53 (encoded by RB1 and TP53, respectively) were then detected by qRT-PCR and western blotting, respectively. At the mRNA level (**Figure 7B**), β-elemene upregulated RB1 and TP53 in a dose-dependent manner from 5 μg/mL onwards in both A549 and NCI-H1650 cells. At 10 and 20 μg/mL, β-elemene exerted a time-dependent effect on RB1 and TP53 levels in A549 cells. In NCI-H1650 cells, a time-dependent effect was observed at different doses for each gene. Similar trends were observed at the protein level (**Figure 7C**). Specifically, dose-and time-dependent effects of β-elemene on pRb and p53 expression were apparent, starting at 2 μg/mL in both cell lines. Collectively, these results indicate that RB1 and TP53, which are both tumor suppressor genes, are target genes of β-elemene in the therapeutic treatment of NSCLC.

β-elemene enhanced the therapeutic effect of cisplatin on NSCLC tumor development and growth in vivo

The combined effect of β-elemene and cisplatin on NSCLC tumor growth was evaluated in an *in vivo* nude mouse xenograft model. A549 cells were subcutaneously injected into experimental mice (n = 6 per treatment group), which were then treated with cisplatin and/or β-elemene. On day 28 of the experiment, the

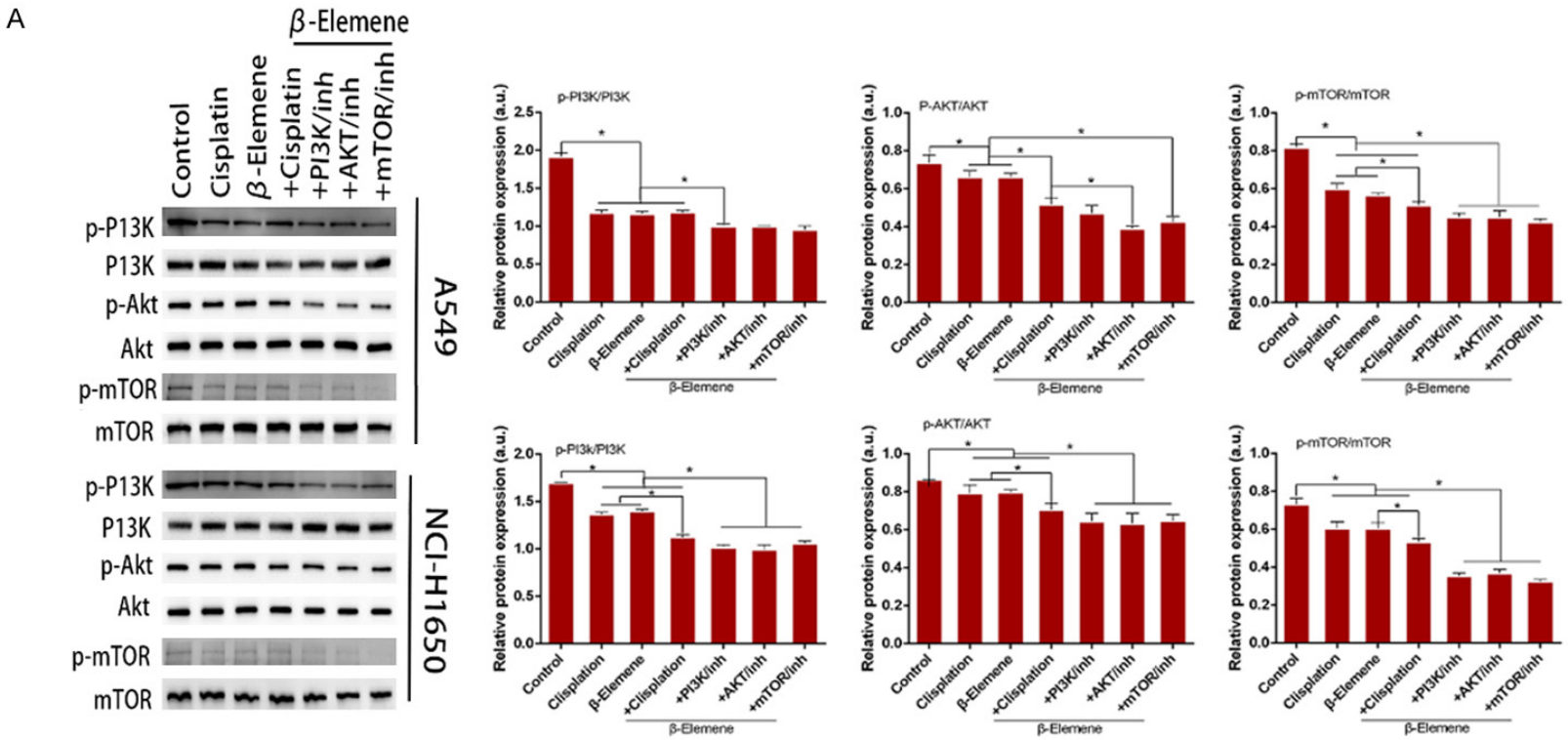
A
β-Elemene
Control
Cisplatin
β-Elemene
+Cisplatin
+PI3K/inh
+AKT/inh
+mTOR/inh
p-P13K
P13K
p-Akt
Akt
p-mTOR
mTOR
A549
NCI-H1650
p-PI3K/PI3K
P-AKT/AKT
p-mTOR/mTOR
p-PI3k/PI3K
p-AKT/AKT
Relative protein expression (a.u.)
β-Elemene

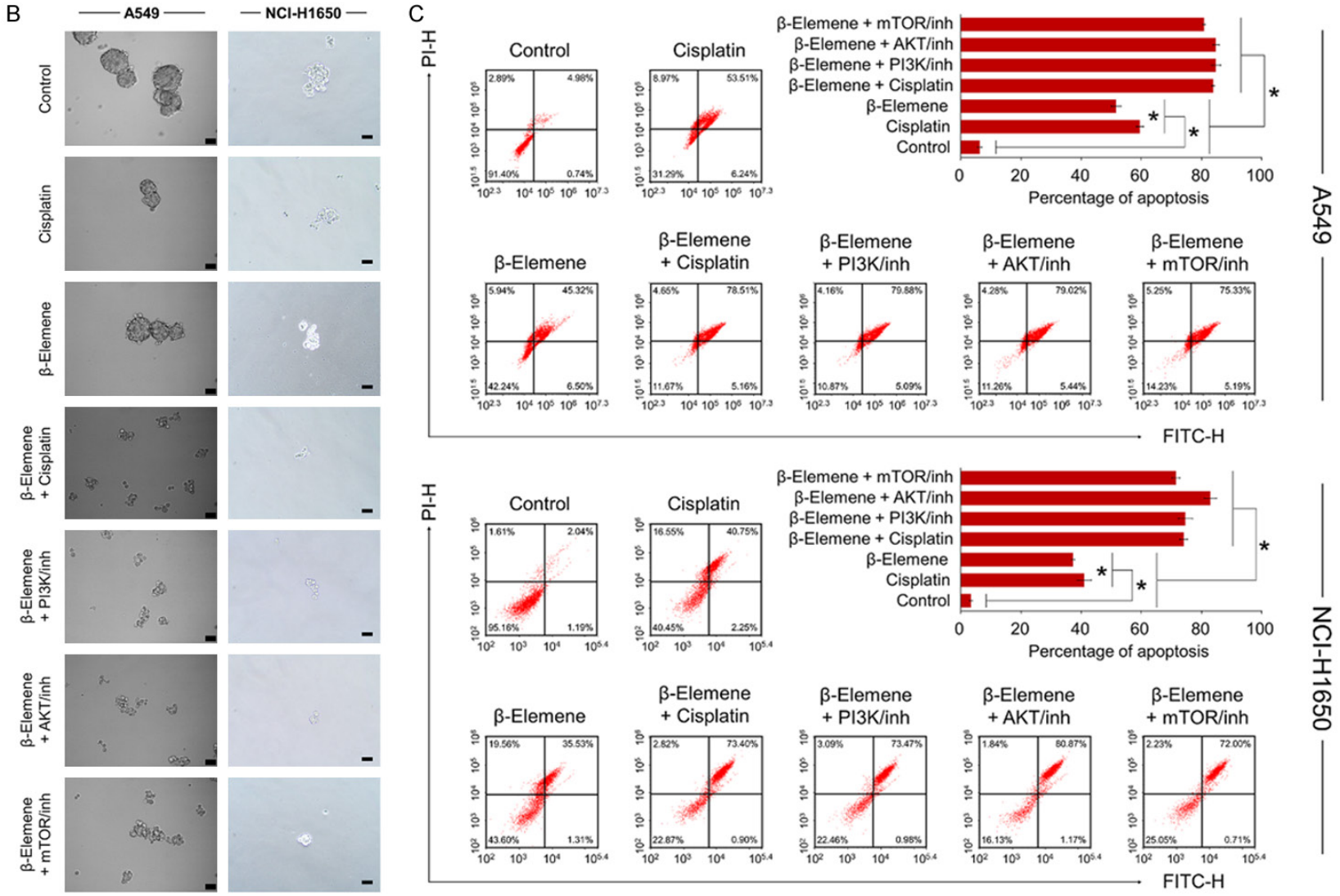

Figure 5. Effect of β-elemene on stemness maintenance and tumorsphere formation in A549 and NCI-H1650 cells in the presence of PI3K/AKT/mTOR inhibitors. A549 and NCI-H1650 cells were treated with 10 μM cisplatin and/or 3 μg/mL β-elemene for 24 h, or first with an inhibitor of PI3K (LY294002, 50 μM), AKT (GSK690693, 10 μM), or mTOR (AZD8055, 10 μM) for 6 h and then with 3 μg/mL β-elemene for 24 h. A. Western blot and quantification of the phosphorylation level of PI3K, AKT, and mTOR relative to total content of respective protein in A549 and NCI-H1650 cells. B. Tumorsphere formation ability of A549 and NCI-H1650 cells. Scale bar = 50 μm. C. Flow cytometry of A549 and NCI-H1650 cell apoptosis after exposure to cisplatin with or without β-elemene at the noted concentrations. Early apoptotic cells are shown in the bottom right quadrant and late apoptotic cells are shown in the top right quadrant. Bar graphs represent the sum of the percentages of early and late apoptotic cells. The data represent the mean ± SD (n = 3), *P < 0.05.

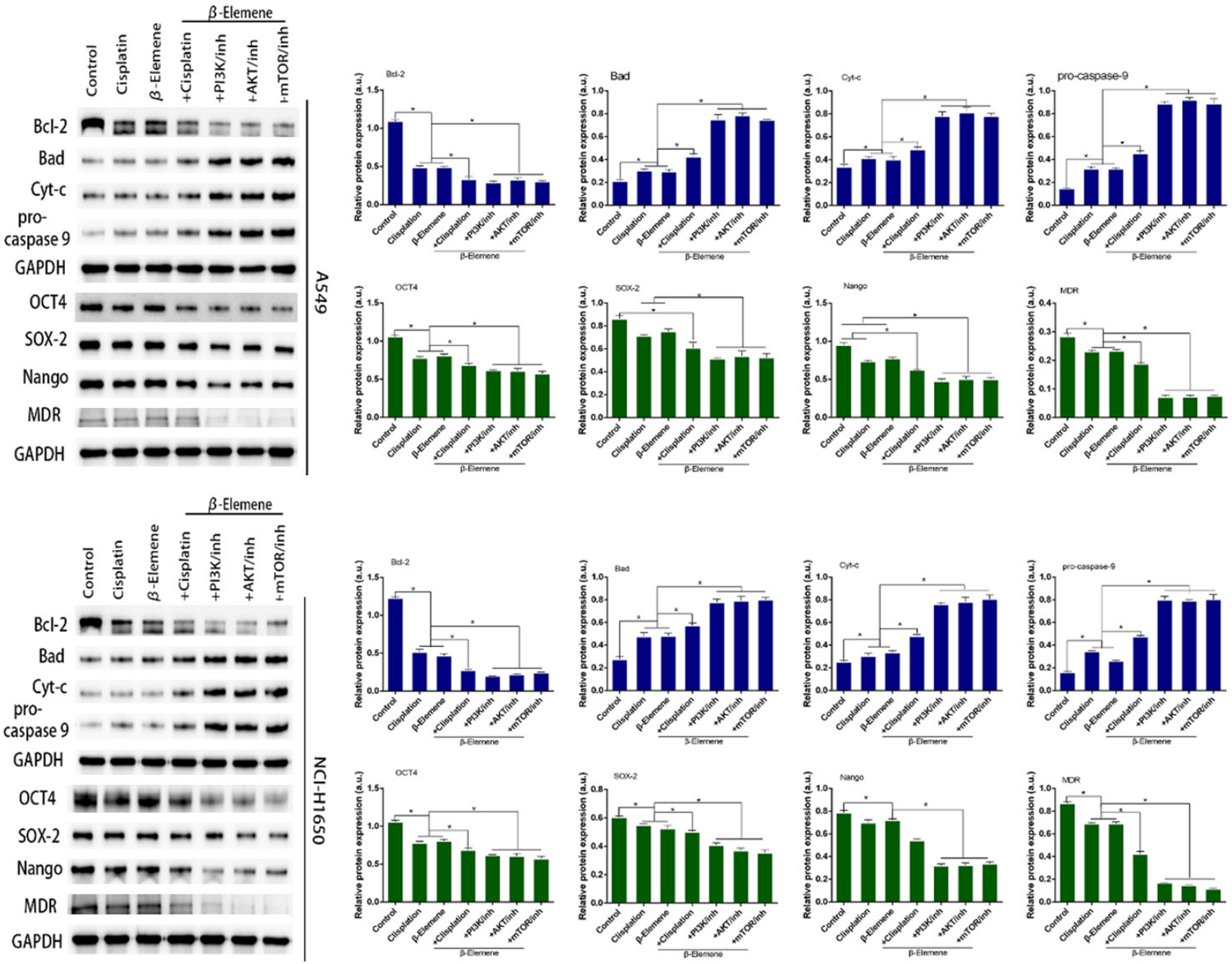
β-Elemene
Control
Cisplatin
β-Elemene
+Cisplatin
+PI3K/inh
+AKT/inh
+mTOR/inh
Bcl-2
Bad
Cyt-c
pro-caspase 9
GAPDH
OCT4
SOX-2
Nango
MDR
GAPDH
A549
NCI-H1650
Relative protein expression (a.u.)
β-Elemene

Figure 6. Effect of β-elemene on apoptosis, stemness, and PI3K/AKT/mTOR signaling in the presence of PI3K/AKT/mTOR inhibitors. A549 and NCI-H1650 cells were treated with 10 μM cisplatin and/or 3 μg/mL for 24 h, or first with an inhibitor of PI3K (LY294002, 50 μM), AKT (GSK690693, 10 μM), or mTOR (AZD8055, 10 μM) for 6 h and then with 3 μg/mL β-elemene for 24 h. Western blot and quantification of the expression of proteins associated with apoptosis (Bcl-2, Bad, Cyt-c, and pro-caspase 9) and stemness maintenance (OCT4, SOX2, and Nanog) in A549 and NCI-H1650 cells. The data represent the mean ± SD (n = 3), *P < 0.05.

Table 1. Names and gene symbols of the predicted targets of β-elemene

Name	Symbol	Node degree
Prostaglandin G/H synthase 2	PTGS2	4
Gamma-aminobutyric-acid receptor alpha-2 subunit	GABRA2	5
Retinoic acid receptor RXR-alpha	RXRA	3
Sodium-dependent noradrenaline transporter	SLC6A2	1
Gamma-aminobutyric-acid receptor alpha-3 subunit	GABRA3	4
Muscarinic acetylcholine receptor M2	CHRM2	4
Gamma-aminobutyric acid receptor subunit alpha-1	GABRA1	5
Gamma-aminobutyric-acid receptor subunit alpha-6	GABRA6	6
Prostaglandin G/H synthase 1	PTGS1	1
Muscarinic acetylcholine receptor M3	CHRM3	3
Muscarinic acetylcholine receptor M1	CHRM1	5
Alpha-1A adrenergic receptor	ADRA1A	3
Neuronal acetylcholine receptor protein, alpha-7 chain	CHRNA7	3
Nuclear receptor coactivator 2	NCOA2	2
Gamma-aminobutyric-acid receptor alpha-5 subunit	GABRA5	5
Apoptosis regulator Bcl-2	BCL2	3
Cyclin-dependent kinase inhibitor 1	CDK1	6
Eukaryotic translation initiation factor 6	EIF6	0
Retinoblastoma-associated protein	RB1	3
Cellular tumor antigen p53	TP53	9
Telomerase protein component 1	TEP1	1
Protein CBFA2T1	RUNX1T1	1
Cell division control protein 2 homolog	CDC2	0
G2/mitotic-specific cyclin-B1	CCNB1	5
Transforming protein RhoA	RHOA	4

tumors were excised for characterization. Visually, individual cisplatin or β-elemene treatments greatly reduced the size of the tumors, and the combined administration of the two further suppressed tumor growth (**Figure 8A**). This was supported by measurements of tumor volume over the 28-day observation period (**Figure 8B**) and tumor weight after the mice were sacrificed on day 28 (**Figure 8C**)-both of which showed sharp decreases with cisplatin and/or β-elemene treatment. Extracted tumor tissues were then subjected to western blotting to detect proteins associated with apoptosis (**Figure 8D**), stemness maintenance (**Figure 8E**), MDR (**Figure 8F**), and PI3K/AKT/mTOR activation (**Figure 8G**). These results were consistent with those obtained *in vitro*. Specifically, the individual administration of cisplatin or β-elemene significantly promoted the apoptosis of tumor cells while suppressing their stem-like properties, MDR ability, and PI3K/AKT/mTOR activation. In all cases, the two drugs exhibited a significantly greater effect when administered in combination than when administered individually.

Discussion

Chemoresistance remains a severe challenge in cancer treatment and hinders effective therapy, resulting in poor prognosis and survival. To address this issue, various targets have been considered, among which CSCs and tumor metabolism have been highlighted in oncology research. Genes such as OCT4, SOX2, and Nanog play an important role in the development of human embryos [27], and are also important for maintaining the stemness of CSCs, wherein these genes are highly expressed [28]. Activation of the PI3K/AKT pathway upregulates the expression of OCT4 and Nanog and promotes the maintenance of breast CSC stemness [29]. Inhibition of OCT4 and Nanog expression inhibits the self-renewal of pancreatic CSCs, enhances the sensitivity of cells to gemcitabine, and promoted apoptosis [30]. PI3K/AKT/mTOR signaling is abnormally activated in various tumor cells, including lung cancer, thereby mediating the occurrence, development, and MDR of tumor cells [31, 32]. This pathway also plays a vital role in mediating the Warburg effect in tumor cells by regulating

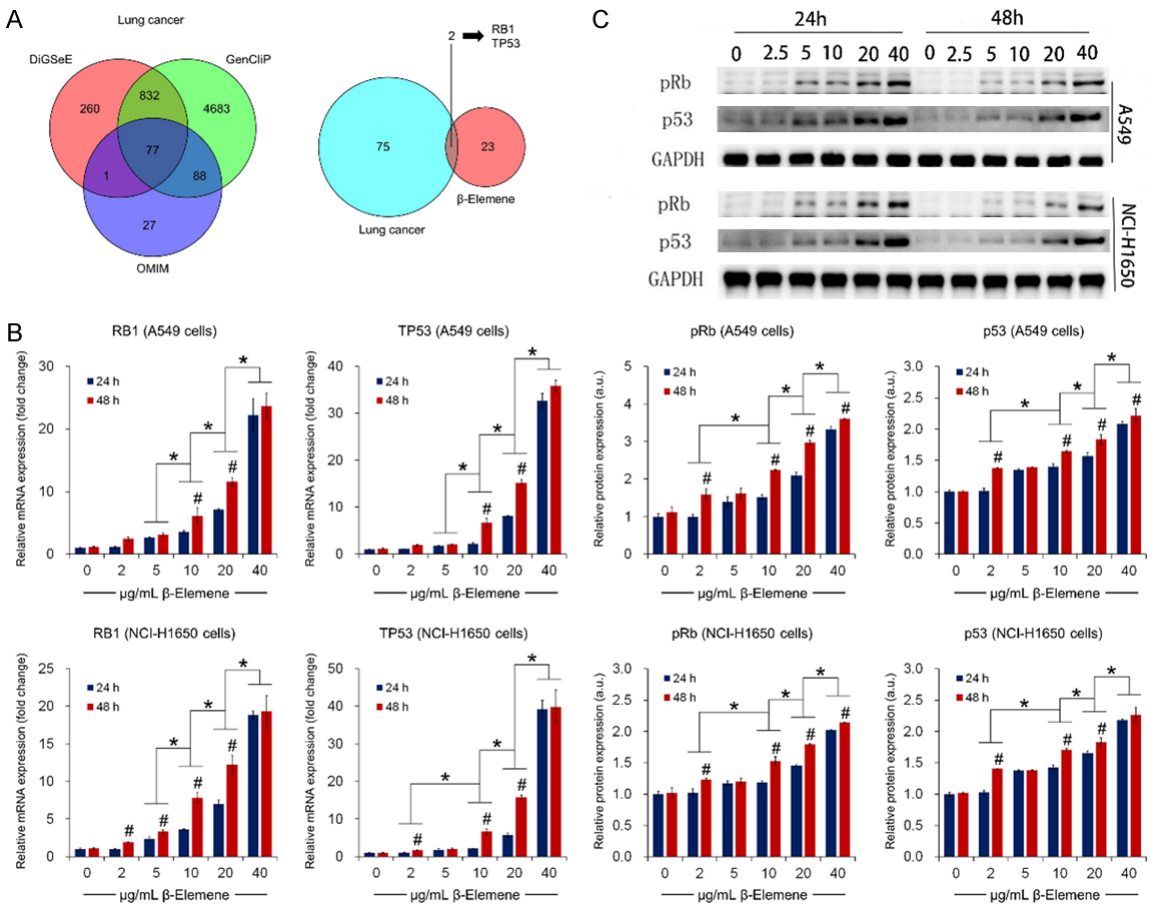

Figure 7. Bioinformatic prediction and experimental validation of target genes of lung cancer and β-elemene. A. Left: venn diagram illustrating the number of target genes associated with lung cancer, identified using DiGSeE, GenCliP, and OMIM. Between the three databases, 77 common genes were found. Right: venn diagram illustrating the number of common target genes associated with both lung cancer and β-elemene. Two target genes (RB1 and TP53) were identified. B. qRT-PCR of the relative mRNA expression of the identified target genes RB1 and TP53 in A549 and NCI-H1650 cells treated with 0, 2, 5, 10, 20, or 40 μg/mL β-elemene for 24 or 48 h. C. Western blot and quantification of the expression of pRb (protein coded by RB1) and p53 (protein coded by TP53) in A549 and NCI-H1650 cells treated with 0, 2, 5, 10, 20, or 40 μg/mL β-elemene for 24 or 48 h. Data represent the mean ± SD (n = 3), *P < 0.05; #P < 0.05 vs. 24 h at the same concentration of β-elemene.

the expression of glycolytic enzymes including GLUT1, HK, LDH, and pyruvate kinase isozyme M2 [33, 34]. AKT has been shown to promote glucose consumption and aerobic glycolysis to enhance tumor growth and survival, exacerbating the malignant behavior of tumor cells [35]. Thus, PI3K/AKT/mTOR has become a well-recognized therapeutic target for various cancers, including NSCLC. The fact that β-elemene suppressed the activation of PI3K, AKT, and mTOR in this study indicates its role as a PI3K/AKT/mTOR inhibitor. Its effects were thus similar to those of chemical inhibitors of PI3K, AKT, and mTOR (LY294002, GSK690693, and AZD8055, respectively) in promoting apoptosis, impairing stemness maintenance, and suppressing MDR.

Conventional chemotherapeutic drugs against NSCLC, such as cisplatin, may cause adverse side effects such as kidney toxicity and ototoxicity. Moreover, MDR poses a significant disadvantage to the efficacy of these drugs. Adjuvant therapy is a promising approach that addresses these issues by using a secondary pharmacological agent to modify or accentuate the effects of chemotherapeutic drugs. Therefore, TCM is considered an attractive option. Owing to the herbal nature of most TCM ingredients, they cause few side effects and are effective in maintaining and improving general health. Therapeutic agents in TCM are often composed of a large number of active natural ingredients; thus, to ensure effective therapeutic use, it is

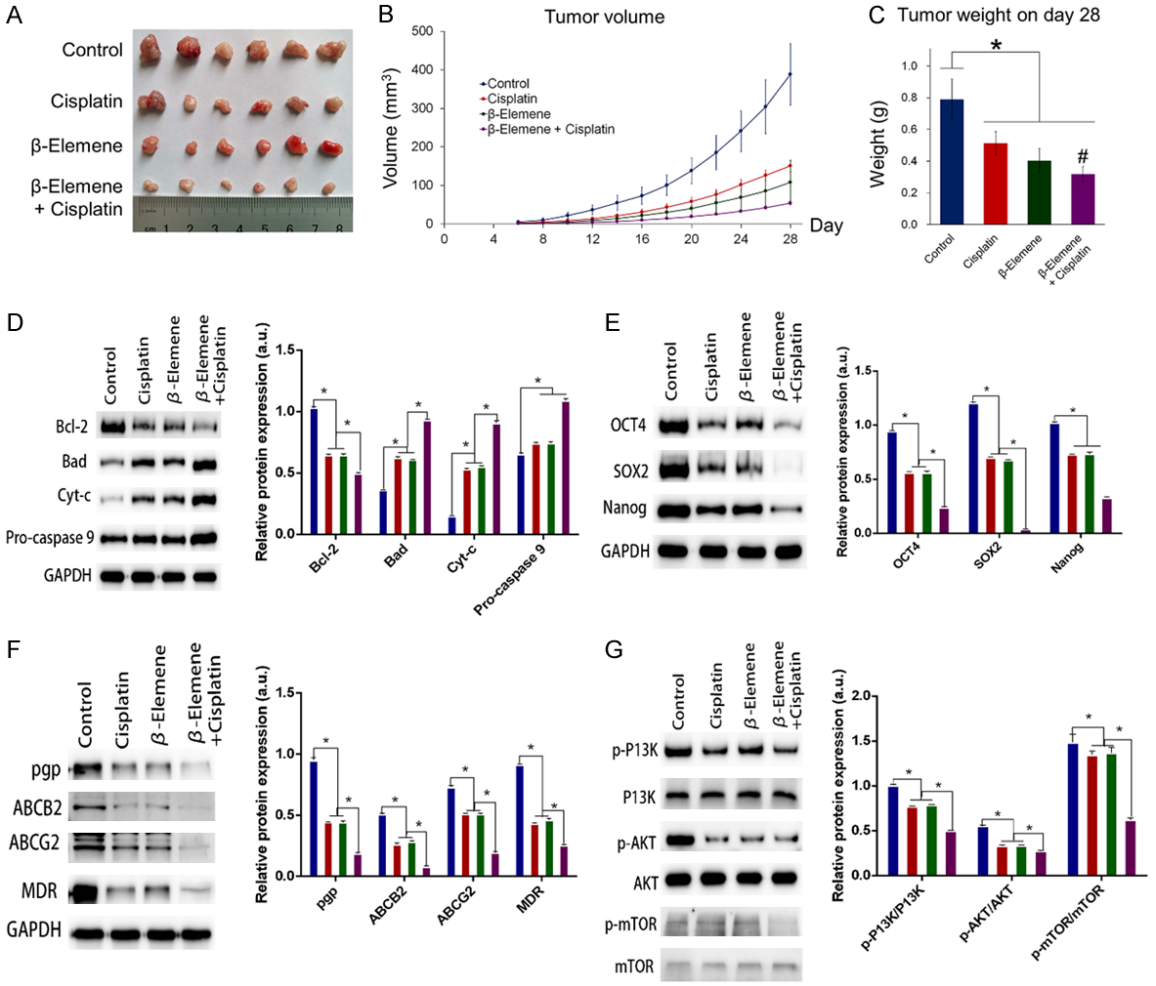

Figure 8. Effect of β-elemene in *in vivo* lung cancer model. (A) Tumors extracted from experimental animals after 28 days of tumor growth (induced by A549 cells), with or without the administration of cisplatin at 5 mg/kg every three days for three weeks and/or β-elemene at 5 mg/kg daily for seven days. (B) Tumor volume monitored over 28-day experimental period. Volume was calculated as (tumor length) × (tumor width)^2 ÷ 2. The data represent the mean ± SD (n = 6). (C) Tumor weight measured on day 28. The data represent the mean ± SD (n = 6), *P < 0.05; #P < 0.05 vs. Cisplatin only. Western blot and quantification of the expression of proteins related to (D) apoptosis (Bcl-2, Bad, Cyt-c, and pro-caspase 9), (E) stemness maintenance (OCT4, SOX2, and Nanog), (F) multi-drug resistance (pgp, ABCB2, ABCG2, and MDR), and (G) PI3K/AKT/mTOR signaling (phosphorylation vs. total protein content) in tumor tissues. The data represent the mean ± SD (n = 6), *P < 0.05.

necessary to precisely identify and characterize the functions and properties of the individual components. In terms of anticancer properties, studies have found that TCM components such as ginsenosides and celastrol can inhibit the proliferation of CSCs and improve the therapeutic effect of chemotherapeutic drugs [36, 37]. Celastrol has also been shown to inhibit the proliferation of gastric cancer cells by disrupting their energy metabolism [38], suggesting that TCM and its main components partially function by targeting the Warburg effect.

The therapeutic effect of β-elemene in NSCLC has been previously demonstrated. Wang et al. reported the mechanism of β-elemene in NSCLC, showing that it promotes apoptosis in NSCLC cells via a mitochondria-mediated pathway [12]. Furthermore, β-elemene acts as an adjuvant agent and exerts synergistic effects with established chemotherapeutic drugs to combat lung cancer. In particular, co-administration of β-elemene and gefitinib, an epidermal growth factor receptor-tyrosine kinase inhibitor, exerted superior antitumor properties to those of the individual components. This was achieved by targeting the stem-like properties of lung cancer cells, disrupting the epithelial-mesenchymal transition, and inhibiting tumor progression *in vivo* through the regulation of

the enhancer of zeste homolog 2 [39]. Similarly, β-elemene exerts synergistic antitumor effects with chemotherapeutic taxanes, including paclitaxel and docetaxel, on lung cancer cells by triggering p53- and Fas-independent pathways and disrupting cell membrane permeability, thereby promoting taxane uptake [40].

Herein, we describe the mechanism by which β-elemene acts as a complementary agent to cisplatin in the treatment of NSCLC. Defects in apoptotic cell death pathways are known to contribute to chemoresistance in tumors [41], wherein high Bcl-2 expression is a strong influencing factor [42]. Although cisplatin significantly downregulated the expression of Bcl-2 in A549 cells and xenografted tumor tissues in this study, this effect was prominently accentuated by β-elemene, showing its unique potential as an antitumor agent. Importantly, β-elemene exerted effects similar to those of the glucose inhibitor 2-DG in altering tumor metabolism. This is a substantial finding because the development of chemoresistance has been critically linked to abnormal glucose metabolism and metabolic reprogramming [43, 44]. Kikuchi et al. presented a well-designed study that revealed the impact of CO_2 levels on mitochondrial metabolism and chemosensitivity. They reported that high CO_2 levels (hypercapnia) are conducive to cisplatin resistance in A549 cells by altering the state of mitochondrial respiration, thereby attenuating reactive oxygen species production [45]. In future studies, it will be interesting to investigate whether the additive effect of β-elemene in complementing cisplatin is influenced by microenvironmental CO_2 levels.

Finally, analysis of the predicted target genes using well-established databases revealed that RB1 and TP53 are associated with both lung cancer and β-elemene. RB1 and TP53 (genes that encode pRb and p53 proteins) are widely considered tumor suppressors. In particular, mutations in RB1 have been correlated with NSCLC and triple-negative breast cancer [46], and p53 is tightly linked to drug resistance and chemotherapy failure [47]. The relationship between PI3K/AKT/mTOR signaling and RB1 or TP53 has also drawn attention for targeted treatment. Notably, mutations in the RB1 pathway lead to the overexpression of mTOR and the phosphorylation of AKT, with critical implications for cell proliferation, cell cycle regulation, apoptosis, and protein synthesis [48]. In terms of TP53 (or p53), numerous studies have reported its tumor-suppressing effects through the inhibition of PI3K/AKT/mTOR signaling [49-51]. The specific roles of RB1 and TP53 in the regulation of MDR by β-elemene via the PI3K/AKT/mTOR pathway remain unknown and will form the basis of prospective research.

Conclusions

Collectively, this study supports the utility of β-elemene as a natural complementary agent to cisplatin for the treatment of NSCLC. Specifically, the underlying mechanisms are associated with the impairment of tumor glucose metabolism, suppression of stem-like properties within the cancer cell population, and inhibition of drug resistance-all of which occur via inactivation of the PI3K/AKT/mTOR signaling pathway. These findings suggest that β-elemene can be considered as an effective clinical adjuvant to conventional chemotherapeutic drugs against lung cancer.

Disclosure of conflict of interest

None.

Address correspondence to: Yan Leng, Department of Encephalopathy, Affiliated Hospital to Changchun University of Chinese Medicine, No. 1478 Gongnong Road, Changchun 130021, Jilin, China. E-mail: 1289021445@qq.com

References

[1] Siegel RL, Miller KD and Jemal A. Cancer statistics, 2018. CA Cancer J Clin 2018; 68: 7-30.

[2] Zarogoulidis K, Zarogoulidis P, Darwiche K, Boutsikou E, Machairiotis N, Tsakiridis K, Katsikogiannis N, Kougioumtzi I, Karapantzos I, Huang H and Spyratos D. Treatment of non-small cell lung cancer (NSCLC). J Thorac Dis 2013; 5 Suppl 4: S389-396.

[3] Luo YH, Luo L, Wampfler JA, Wang Y, Liu D, Chen YM, Adjei AA, Midthun DE and Yang P. 5-year overall survival in patients with lung cancer eligible or ineligible for screening according to US preventive services task force criteria: a prospective, observational cohort study. Lancet Oncol 2019; 20: 1098-1108.

[4] Simeone JC, Nordstrom BL, Patel K and Klein AB. Treatment patterns and overall survival in metastatic non-small-cell lung cancer in a real-world, US setting. Future Oncol 2019; 15: 3491-3502.

[5] Holohan C, Van Schaeybroeck S, Longley DB and Johnston PG. Cancer drug resistance: an evolving paradigm. Nat Rev Cancer 2013; 13: 714-726.
[6] Clarke MF, Dick JE, Dirks PB, Eaves CJ, Jamieson CH, Jones DL, Visvader J, Weissman IL and Wahl GM. Cancer stem cells--perspectives on current status and future directions: AACR workshop on cancer stem cells. Cancer Res 2006; 66: 9339-9344.
[7] Adorno-Cruz V, Kibria G, Liu X, Doherty M, Junk DJ, Guan D, Hubert C, Venere M, Mulkearns-Hubert E, Sinyuk M, Alvarado A, Caplan AI, Rich J, Gerson SL, Lathia J and Liu H. Cancer stem cells: targeting the roots of cancer, seeds of metastasis, and sources of therapy resistance. Cancer Res 2015; 75: 924-929.
[8] Pattabiraman DR and Weinberg RA. Tackling the cancer stem cells-what challenges do they pose? Nat Rev Drug Discov 2014; 13: 497-512.
[9] Vander Heiden MG, Cantley LC and Thompson CB. Understanding the Warburg effect: the metabolic requirements of cell proliferation. Science 2009; 324: 1029-1033.
[10] Xia P and Xu XY. PI3K/Akt/mTOR signaling pathway in cancer stem cells: from basic research to clinical application. Am J Cancer Res 2015; 5: 1602-1609.
[11] Long J, Liu Z and Hui L. Anti-tumor effect and mechanistic study of elemene on pancreatic carcinoma. BMC Complement Altern Med 2019; 19: 133.
[12] Wang G, Li X, Huang F, Zhao J, Ding H, Cunningham C, Coad JE, Flynn DC, Reed E and Li QQ. Antitumor effect of beta-elemene in non-small-cell lung cancer cells is mediated via induction of cell cycle arrest and apoptotic cell death. Cell Mol Life Sci 2005; 62: 881-893.
[13] Zhang X, Li Y, Zhang Y, Song J, Wang Q, Zheng L and Liu D. Beta-elemene blocks epithelial-mesenchymal transition in human breast cancer cell line MCF-7 through Smad3-mediated down-regulation of nuclear transcription factors. PLoS One 2013; 8: e58719.
[14] Wu XS, Xie T, Lin J, Fan HZ, Huang-Fu HJ, Ni LF and Yan HF. An investigation of the ability of elemene to pass through the blood-brain barrier and its effect on brain carcinomas. J Pharm Pharmacol 2009; 61: 1653-1656.
[15] Zhai B, Zeng Y, Zeng Z, Zhang N, Li C, Zeng Y, You Y, Wang S, Chen X, Sui X and Xie T. Drug delivery systems for elemene, its main active ingredient beta-elemene, and its derivatives in cancer therapy. Int J Nanomedicine 2018; 13: 6279-6296.
[16] Wang QT, Zhang ZL, Xiong H, Zhou DS, Li J, Liang J and Wang YF. Evaluation of the efficacy and safety of elemene in treating malignant pleural effusion caused by tumors: a PRISMA guided meta-analysis. Medicine (Baltimore) 2018; 97: e12542.
[17] Zheng C, Cai X, Wu S, Liu Z, Shi Y and Zhou W. Enhancing effect of beta-elemene emulsion on chemotherapy with harringtonine, aclacinomycin, and Ara-c in treatment of refractory/relapsed acute myeloid leukemia. Pak J Med Sci 2014; 30: 1270-1272.
[18] Li X, Wang G, Zhao J, Ding H, Cunningham C, Chen F, Flynn DC, Reed E and Li QQ. Antiproliferative effect of beta-elemene in chemoresistant ovarian carcinoma cells is mediated through arrest of the cell cycle at the G2-M phase. Cell Mol Life Sci 2005; 62: 894-904.
[19] Guan C, Liu W, Yue Y, Jin H, Wang X and Wang XJ. Inhibitory effect of beta-elemene on human breast cancer cells. Int J Clin Exp Pathol 2014; 7: 3948-3956.
[20] Wu Z, Wang T, Zhang Y, Zheng Z, Yu S, Jing S, Chen S, Jiang H and Ma S. Anticancer effects of beta-elemene with hyperthermia in lung cancer cells. Exp Ther Med 2017; 13: 3153-3157.
[21] Jiang X, Hidru TH, Zhang Z, Bai Y, Kong L and Li X. Evidence of elemene injection combined radiotherapy in lung cancer treatment among patients with brain metastases: a systematic review and meta-analysis. Medicine (Baltimore) 2017; 96: e6963.
[22] Liu S, Zhou L, Zhao Y and Yuan Y. Beta-elemene enhances both radiosensitivity and chemosensitivity of glioblastoma cells through the inhibition of the ATM signaling pathway. Oncol Rep 2015; 34: 943-951.
[23] Li CL, Chang L, Guo L, Zhao D, Liu HB, Wang QS, Zhang P, Du WZ, Liu X, Zhang HT, Liu Y, Zhang Y, Xie JH, Ming JG, Cui YQ, Sun Y, Zhang ZR and Jiang CL. Beta-elemene induces caspase-dependent apoptosis in human glioma cells in vitro through the upregulation of Bax and Fas/FasL and downregulation of Bcl-2. Asian Pac J Cancer Prev 2014; 15: 10407-10412.
[24] Zhan YH, Liu J, Qu XJ, Hou KZ, Wang KF, Liu YP and Wu B. Beta-elemene induces apoptosis in human renal-cell carcinoma 786-0 cells through inhibition of MAPK/ERK and PI3K/Akt/mTOR signalling pathways. Asian Pac J Cancer Prev 2012; 13: 2739-2744.
[25] Zhu TZ, Li XM, Luo LH, Song ZQ, Gao X, Li ZQ, Su JY and Liang GB. Beta-elemene inhibits stemness, promotes differentiation and impairs chemoresistance to temozolomide in glioblastoma stem-like cells. Int J Oncol 2014; 45: 699-709.
[26] Crous AM and Abrahamse H. Lung cancer stem cells and low-intensity laser irradiation: a po-

tential future therapy? Stem Cell Res Ther 2013; 4: 129.
[27] Wu G and Scholer HR. Role of Oct4 in the early embryo development. Cell Regen (Lond) 2014; 3: 7.
[28] Liu A, Yu X and Liu S. Pluripotency transcription factors and cancer stem cells: small genes make a big difference. Chin J Cancer 2013; 32: 483-487.
[29] Almozyan S, Colak D, Mansour F, Alaiya A, Al-Harazi O, Qattan A, Al-Mohanna F, Al-Alwan M and Ghebeh H. PD-L1 promotes OCT4 and Nanog expression in breast cancer stem cells by sustaining PI3K/AKT pathway activation. Int J Cancer 2017; 141: 1402-1412.
[30] Lu Y, Zhu H, Shan H, Lu J, Chang X, Li X, Lu J, Fan X, Zhu S, Wang Y, Guo Q, Wang L, Huang Y, Zhu M and Wang Z. Knockdown of Oct4 and Nanog expression inhibits the stemness of pancreatic cancer cells. Cancer Lett 2013; 340: 113-123.
[31] Yip PY. Phosphatidylinositol 3-kinase-AKT-mammalian target of rapamycin (PI3K-Akt-mTOR) signaling pathway in non-small cell lung cancer. Transl Lung Cancer Res 2015; 4: 165-176.
[32] Cheng H, Shcherba M, Pendurti G, Liang Y, Piperdi B and Perez-Soler R. Targeting the PI3K/AKT/mTOR pathway: potential for lung cancer treatment. Lung Cancer Manag 2014; 3: 67-75.
[33] Zha X, Sun Q and Zhang H. MTOR upregulation of glycolytic enzymes promotes tumor development. Cell Cycle 2011; 10: 1015-1016.
[34] Sun Q, Chen X, Ma J, Peng H, Wang F, Zha X, Wang Y, Jing Y, Yang H, Chen R, Chang L, Zhang Y, Goto J, Onda H, Chen T, Wang MR, Lu Y, You H, Kwiatkowski D and Zhang H. Mammalian target of rapamycin up-regulation of pyruvate kinase isoenzyme type M2 is critical for aerobic glycolysis and tumor growth. Proc Natl Acad Sci U S A 2011; 108: 4129-4134.
[35] Elstrom RL, Bauer DE, Buzzai M, Karnauskas R, Harris MH, Plas DR, Zhuang H, Cinalli RM, Alavi A, Rudin CM and Thompson CB. Akt stimulates aerobic glycolysis in cancer cells. Cancer Res 2004; 64: 3892-3899.
[36] Tang YC, Zhang Y, Zhou J, Zhi Q, Wu MY, Gong FR, Shen M, Liu L, Tao M, Shen B, Gu DM, Yu J, Xu MD, Gao Y and Li W. Ginsenoside Rg3 targets cancer stem cells and tumor angiogenesis to inhibit colorectal cancer progression in vivo. Int J Oncol 2018; 52: 127-138.
[37] Moreira H, Szyjka A and Gasiorowski K. Chemopreventive activity of celastrol in drug-resistant human colon carcinoma cell cultures. Oncotarget 2018; 9: 21211-21223.
[38] Wang SJ, Dong LQ, Liu H, Zhao JK, Sun WW, Ren S and Zhang H. Effect of celastrol on antiproliferation and energy metabolism in SGC-7901 cells and ECV304 cells. Chinese Traditional and Herbal Drugs 2016; 47: 3854-3860.
[39] Cheng H, Ge X, Zhuo S, Gao Y, Zhu B, Zhang J, Shang W, Xu D, Ge W and Shi L. Beta-elemene synergizes with gefitinib to inhibit stem-like phenotypes and progression of lung cancer via down-regulating EZH2. Front Pharmacol 2018; 9: 1413.
[40] Zhao J, Li QQ, Zou B, Wang G, Li X, Kim JE, Cuff CF, Huang L, Reed E and Gardner K. In vitro combination characterization of the new anticancer plant drug beta-elemene with taxanes against human lung carcinoma. Int J Oncol 2007; 31: 241-252.
[41] Hajra KM and Liu JR. Apoptosome dysfunction in human cancer. Apoptosis 2004; 9: 691-704.
[42] Reed JC. Regulation of apoptosis by bcl-2 family proteins and its role in cancer and chemoresistance. Curr Opin Oncol 1995; 7: 541-546.
[43] Zhao F, Mancuso A, Bui TV, Tong X, Gruber JJ, Swider CR, Sanchez PV, Lum JJ, Sayed N, Melo JV, Perl AE, Carroll M, Tuttle SW and Thompson CB. Imatinib resistance associated with BCR-ABL upregulation is dependent on HIF-1alpha-induced metabolic reprograming. Oncogene 2010; 29: 2962-2972.
[44] Kominsky DJ, Klawitter J, Brown JL, Boros LG, Melo JV, Eckhardt SG and Serkova NJ. Abnormalities in glucose uptake and metabolism in imatinib-resistant human BCR-ABL-positive cells. Clin Cancer Res 2009; 15: 3442-3450.
[45] Kikuchi R, Iwai Y, Tsuji T, Watanabe Y, Koyama N, Yamaguchi K, Nakamura H and Aoshiba K. Hypercapnic tumor microenvironment confers chemoresistance to lung cancer cells by reprogramming mitochondrial metabolism in vitro. Free Radic Biol Med 2019; 134: 200-214.
[46] Gong X, Du J, Parsons SH, Merzoug FF, Webster Y, Iversen PW, Chio LC, Van Horn RD, Lin X, Blosser W, Han B, Jin S, Yao S, Bian H, Ficklin C, Fan L, Kapoor A, Antonysamy S, Mc Nulty AM, Froning K, Manglicmot D, Pustilnik A, Weichert K, Wasserman SR, Dowless M, Marugan C, Baquero C, Lallena MJ, Eastman SW, Hui YH, Dieter MZ, Doman T, Chu S, Qian HR, Ye XS, Barda DA, Plowman GD, Reinhard C, Campbell RM, Henry JR and Buchanan SG. Aurora A Kinase inhibition is synthetic lethal with loss of the RB1 tumor suppressor gene. Cancer Discov 2019; 9: 248-263.
[47] Hientz K, Mohr A, Bhakta-Guha D and Efferth T. The role of p53 in cancer drug resistance and targeted chemotherapy. Oncotarget 2017; 8: 8921-8946.
[48] El-Naggar S, Liu Y and Dean DC. Mutation of the Rb1 pathway leads to overexpression of mTor, constitutive phosphorylation of Akt on

serine 473, resistance to anoikis, and a block in c-Raf activation. Mol Cell Biol 2009; 29: 5710-5717.
[49] Song R, Tian K, Wang W and Wang L. P53 suppresses cell proliferation, metastasis, and angiogenesis of osteosarcoma through inhibition of the PI3K/AKT/mTOR pathway. Int J Surg 2015; 20: 80-87.
[50] Li Y, Wang T, Sun Y, Huang T, Li C, Fu Y, Li Y and Li C. P53-mediated PI3K/AKT/mTOR pathway played a role in Ptox (Dpt)-induced EMT inhibition in liver cancer cell lines. Oxid Med Cell Longev 2019; 2019: 2531493.
[51] Feng Z. P53 regulation of the IGF-1/AKT/mTOR pathways and the endosomal compartment. Cold Spring Harb Perspect Biol 2010; 2: a001057.